





Communication

# Multiplicity Dependence in the Non-Extensive Hadronization Model Calculated by the HIJING++ Framework

Gábor Bíró<sup>1,2,\*†</sup> , Gergely Gábor Barnaföldi<sup>1,\*†</sup> , Gábor Papp<sup>2,\*†</sup>  and Tamás Sándor Biró<sup>1,\*†</sup> 

<sup>1</sup> Wigner Research Centre for Physics of the Hungarian Academy of Sciences, Department of Theory, 29-33 Konkoly-Thege Miklós Str, H-1121 Budapest, Hungary

<sup>2</sup> Institute for Physics, Eötvös Loránd University, 1/A Pázmány P. Sétány, H-1117, Budapest, Hungary

\* Correspondence: biro.gabor@wigner.mta.hu (G.B.); barnafoldi.gergely@wigner.mta.hu (G.G.B.); pg@ludens.elte.hu (G.P.); biro.tamas@wigner.mta.hu (T.S.B.)

† These authors contributed equally to this work.

Received: 30 April 2019; Accepted: 23 May 2019; Published: date

**Abstract:** The non-extensive statistical description of the identified final state particles measured in high energy collisions is well-known by its wide range of applicability. However, there are many open questions that need to be answered, including but not limited to, the question of the observed mass scaling of massive hadrons or the size and multiplicity dependence of the model parameters. This latter is especially relevant, since currently the amount of available experimental data with high multiplicity at small systems is very limited. This contribution has two main goals: On the one hand we provide a status report of the ongoing tuning of the soon-to-be-released HIJING++ Monte Carlo event generator. On the other hand, the role of multiplicity dependence of the parameters in the non-extensive hadronization model is investigated with HIJING++ calculations. We present cross-check comparisons of HIJING++ with existing experimental data to verify its validity in our range of interest as well as calculations at high-multiplicity regions where we have insufficient experimental data.

**Keywords:** high energy physics; heavy-ion; Monte Carlo; event generator; parallel computing; HIJING, non-extensive; Tsallis

## 1. Introduction

The transverse momentum ( $p_T$ ) distribution of identified hadrons stemming from high-energy proton–proton, proton–nucleus, and nucleus–nucleus collisions is one of the most fundamental observables in high-energy physics. In recent years, the Tsallis–Pareto-like distributions, motivated from non-extensive statistical physics, have received close attention because their applicability in this field [1–7]. With the appearance of high precision experimental data spanning from low- to high- $p_T$ , neither the thermal models with a bare Boltzmann–Gibbs exponential distribution nor perturbative Quantum Chromodynamics (pQCD)-motivated power-law distributions are able to describe the whole spectrum. On the other hand, the Tsallis–Pareto distributions combine these two regions perfectly (see, e.g., [1–16] and references therein). During the investigation of the parameters, we showed that they possess non-trivial relations such as mass- and energy scaling [1,8]. There are also implications that for larger systems a *soft-hard* extension is needed [10,16]. These studies indicate that increasing the size of the colliding system (roughly speaking, the volume of the quark-gluon plasma) may also reflect in the parameters. Our goal is therefore to systematically explore the parameter space as the function of the event multiplicity.

The HIJING++ framework is a soon-to-be-published general purpose Monte Carlo event generator, currently in the final phase of development [17–22]. It will serve as the successor of the FORTRAN HIJING,

completely rewritten in modern C++. With the flexibility gained by using modular C++ structures, HIJING++ also utilizes several external packages [23–29]. Currently the internal parameters of HIJING++ are being tuned to main experimental observables using Professor [30,31]. This provides an excellent opportunity to test the capabilities of HIJING++ and calculate high-multiplicity events.

In the next section, we briefly summarize the progress of tuning in HIJING++ and present the current status. In Section 3, a theoretical description of the transverse momentum spectra is given, and the HIJING++ calculations are given in Section 4.

## 2. Tuning of HIJING++ Parameters

A typical general purpose Monte Carlo event generator, e.g., the HIJING++ framework, developed to be able to simulate high-energy heavy-ion collisions, has parameters that are not determined by theory and need to be tuned to reproduce measured experimental data with the highest possible precision. One of the main features of the HIJING++ framework is that very few input parameters are needed to fully define a run, such as the species of the projectile and target beam and center-of-mass energy. Given this information, all of the other intrinsic parameters are calculated automatically.

Since HIJING++ is based on the convolution of sequential collisions of nucleon–nucleon pairs in each nucleus–nucleus interaction, it is highly important to have a solid proton–proton collisions baseline. In this section, we present the up-to-date result of the tuning process using the following  $\sqrt{s} = 7$  TeV proton–proton experimental data:

- $p_T$  spectra of identified  $\pi^\pm$ ,  $K^\pm$ , and  $p(\bar{p})$  hadrons with  $INEL > 0$  normalization (at least one charged particle in the  $|\eta| < 1.0$  region is required) up to  $p_T = 20$  GeV/c [32];
- charged hadron multiplicity distribution in the range of  $\langle dN_{ch}/d\eta \rangle = 0 - 70$ , where  $N_{ch}$  is the number of charged particles [33,34];
- charged hadron  $\eta = \frac{1}{2} \ln \frac{p^+p_Z}{p^-p_{\bar{Z}}}$  pseudorapidity distribution at mid-pseudorapidity  $|\eta| < 1.0$  [33].

The tuning process is performed iteratively utilizing the Professor tool [30,31]. In Table 1, we list the main tunable parameters.

**Table 1.** Main internal parameters in HIJING++.

| Parameter              | Description   |
|------------------------|---|
| $p_0$                  | soft-hard separation scale: minimum $p_T$ transfer of hard or semihard scatterings  |
| $\sigma_{soft}$        | the inclusive cross section for soft interactions   |
| $\sigma_0$             | the cross section that characterizes the geometrical size of a nucleon  |
| $\mu_0$                | the parameter in the scaled eikonal function of nucleon used to calculate total cross-section   |
| $K$                    | K-factor for the differential jet cross sections in the lowest order pQCD calculation   |
| $\max p_{T,cut}$       | $p_T$ cut for classifying the connected-independent type strings at fragmentation   |
| $m_{inv-cut}$          | invariant mass cut-off for the dipole radiation of a string system below which soft gluon radiations are terminated   |
| $m_{min-inv-ex.str.}$  | minimum value for the invariant mass of the excited string system in a hadron-hadron interaction  |
| $S_{p_{T_1}}$          | the parameter that regularizes the singularity at $p_T = 0$ in the distribution of the soft $p_T$ kick  |
| $S_{p_{T_2}}$          | the parameter that gives the scale beyond which the $p_T$ kick distribution will be similar to $1/p_T^4$  |
| $F$                    | the scale in the form factor to suppress the $p_T$ transfer to diquarks in hard scatterings   |
| $v_{q_i}$              | phenomenological parameters ( $i = 1, 2, 3$ ) of the soft parton distribution function that yield an $x$ distribution of the valence quarks in a soft interaction |
| $s_{q_i}$              | phenomenological parameters ( $i = 1, 2, 3$ ) of the soft parton distribution function that yield an $x$ distribution of the sea quarks in a soft interaction     |
| StringPT:temperature   | the temperature parameter in the Lund fragmentation model as described in [23]  |
| StringPT:tempPreFactor | the temperature prefactor for strange quarks and diquarks in the Lund fragmentation model as described in [23]  |
| StringZ:aExtraSQuark   | parameters in the Lund symmetric fragmentation function as described in [23]  |
| StringZ:aExtraDiQuark  |   |

The detailed process of tuning and the parameters values will be described in the technical release paper of HIJING++. Here we present only the tuning status regarding the experimental data listed above.

In Figure 1, the multiplicity and the pseudorapidity distribution of charged hadrons are presented, while in Figure 2 the  $p_T$  spectrum of identified  $\pi^\pm$ ,  $K^\pm$ , and  $p(\bar{p})$  hadrons calculated and measured at  $\sqrt{s} = 7$  TeV proton-proton collisions can be seen.

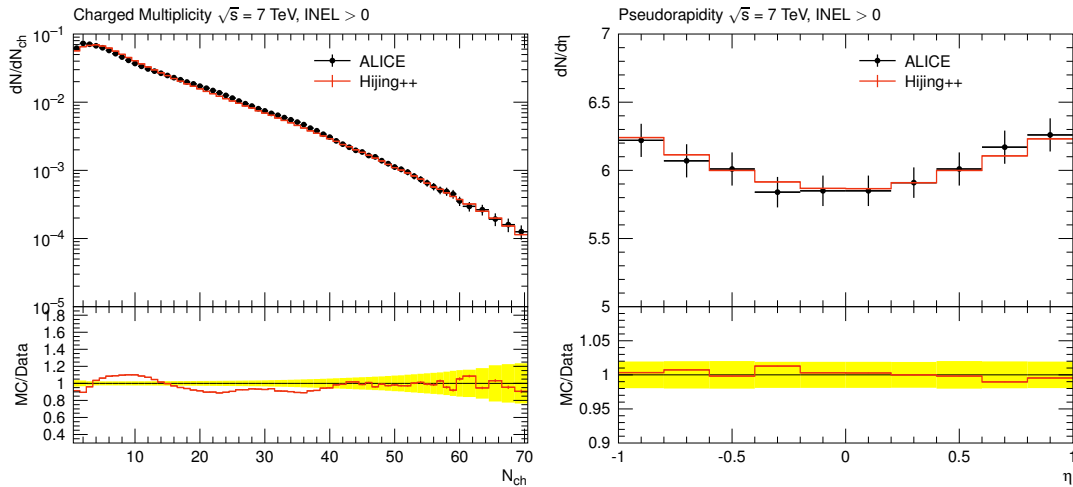


**Figure 1.** The multiplicity distribution (left panel) and pseudorapidity distribution (right panel) of charged hadrons stemming from proton-proton collisions at  $\sqrt{s} = 7$  TeV calculated with HIJING++ and compared to experimental data [33,34].

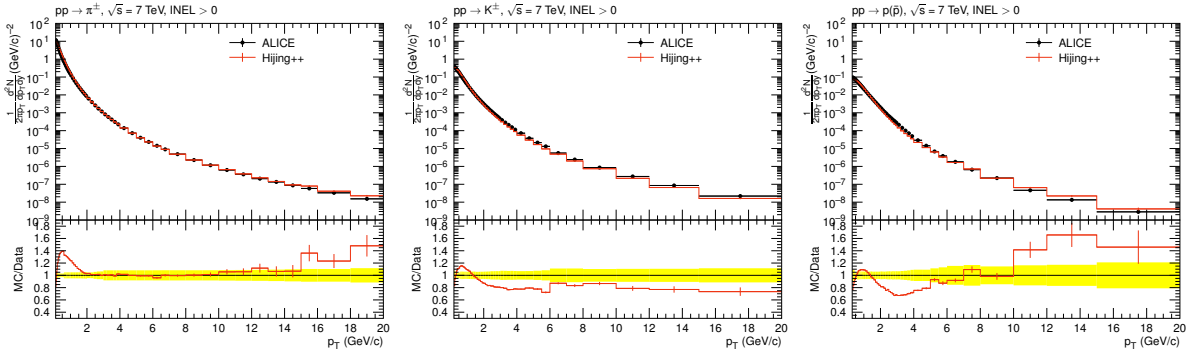


**Figure 2.** The  $p_T$  spectrum of identified  $\pi^\pm$  (left panel),  $K^\pm$  (middle panel), and  $p(\bar{p})$  (right panel) hadrons yield from proton–proton collisions at  $\sqrt{s} = 7$  TeV with  $INEL > 0$  normalization calculated with HIJING++ and compared to experimental data [32].

The results above show that HIJING++ reproduces the event multiplicity excellently. In Figure 1, the agreement between the HIJING++ results and the experimental data is  $\sim 15\%$  for the multiplicity and  $\sim 1\%$  for the pseudorapidity distribution. The charged pion and kaon spectra also show a good agreement above  $p_T = 2$  GeV/c, but the production is slightly overestimated at lower  $p_T$  values. The best agreement for the  $\pi^\pm$  results is  $\sim 1\%$  between 2 and 15 GeV/c. For kaons, the yield is slightly underestimated above 2 GeV/c, where the agreement is  $\sim 15\text{--}20\%$ . On the other hand, the proton yield is overestimated in the large  $p_T$  region, the agreement is  $\sim 20\text{--}30\%$ .

### 3. The Non-Extensive Hadronization Model

It is a well-known and an intensively studied phenomenon that the transverse momentum spectra of hadrons stemming from high-energy particle collisions can be described by Tsallis–Pareto type distributions [1–3,6,8–13]. Although this observation itself has further consequences, the theory has even more subtle details because of the observed non-trivial dependence on the center-of-mass energy and hadron mass. In the following sections, we show that the parameters also depend on the event multiplicity, i.e., on the size of the system.

We adopted the usual blast-wave assumptions regarding the system, namely that the fireball is azimuthally symmetric and is expanding with a  $v$  radial flow velocity (in units of  $c = 1$ ). Moreover, the freeze-out occurs instantly on a hypersurface according to the Cooper–Frye formulation at a given freeze-out temperature [2,14]. With these assumptions, we used the following simple form of the invariant yield:

$$\left. \frac{d^2N}{p_T dp_T dy} \right|_{INEL > 0} = A \cdot m_T \cdot \left( 1 + \frac{E}{nT} \right)^{-n} \quad (1)$$

where  $A$  is the amplitude incorporating the irrelevant spin degeneracy and constant factors as well as the invariant volume,  $m_T = \sqrt{p_T^2 + m^2}$  is the transverse mass,  $E = \gamma(m_T - vp_T) - m$  is the one-particle energy in the co-moving coordinate system,  $\gamma = 1/\sqrt{1 - v^2}$  is the Lorentz factor,  $T$  is a parameter with a temperature unit, and finally  $n = \frac{1}{q-1}$  is the non-extensivity parameter, characterizing the temperature fluctuations. We note that  $T$  is not necessarily the freeze-out temperature and therefore is not necessarily the same for all hadron species [3,15]. The notation  $INEL > 0$  means that only those events where there is at least one charged particle in the  $|\eta| < 1.0$  region are considered. This choice is in agreement with the experimental definitions described in the previous section.

As a reference, in Table 2 and in Figure 3, we show the parameters and curves fitted on the experimental “minimum bias” (in the sense that there is no event multiplicity classification) data. These results are consistent with our previous observations [8]: the heaviest proton has the largest temperature and the smallest  $q$ . We note that, in the lower part of Figure 3, a periodic oscillation is visible. This is an effect in addition to the scaling. This has been investigated, for example, in [35,36].

**Table 2.** Tsallis parameters extracted from “minimum bias”  $INEL > 0$  proton–proton collisions at  $\sqrt{s} = 7$  TeV, measured by ALICE [32]

| Hadron       | $n$               | $q$               | $T$ (GeV)         | $A$                | $v$               | $\chi^2/ndf$ |
|--------------|-------------------|-------------------|-------------------|--------------------|-------------------|--------------|
| $\pi^\pm$    | $7.415 \pm 0.033$ | $1.135 \pm 0.005$ | $0.089 \pm 0.010$ | $73.188 \pm 9.700$ | $0.000 \pm 0.119$ | 174.225 / 54 |
| $K^\pm$      | $7.539 \pm 0.086$ | $1.133 \pm 0.013$ | $0.155 \pm 0.010$ | $0.915 \pm 0.095$  | $0.000 \pm 0.066$ | 20.274 / 47  |
| $p(\bar{p})$ | $8.805 \pm 0.184$ | $1.114 \pm 0.023$ | $0.191 \pm 0.012$ | $0.124 \pm 0.013$  | $0.000 \pm 0.054$ | 18.462 / 45  |

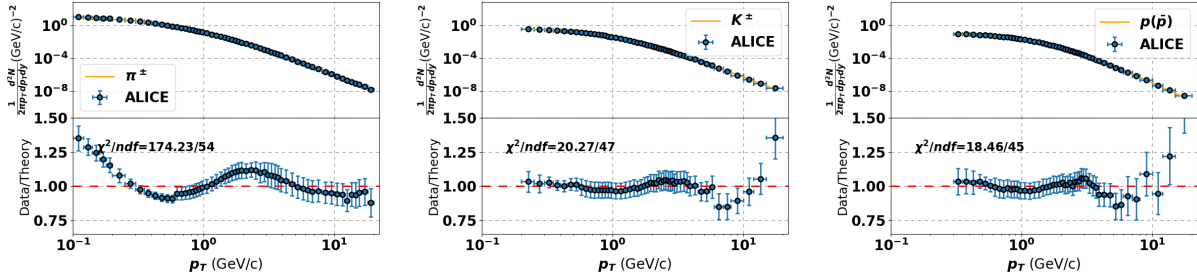


**Figure 3.** Fits of the Tsallis–Pareto distribution to  $\pi^\pm$ ,  $K^\pm$ , and  $p(\bar{p})$  hadrons measured by ALICE [32].

#### 4. The Multiplicity Dependence of the Non-Extensive Model

In Section 2, we showed that the HIJING++ framework is able to reproduce the main experimental observables such as event multiplicity distribution and the  $p_T$  spectra of various identified hadrons. In Section 3, we briefly summarized the main features of the blast-wave motivated non-extensive hadronization model. In this section, we take advantage of the power of HIJING++ and extract the Tsallis parameters from a wide range of event multiplicity classes. The event classes of the HIJING++ run are classified as

$$\text{Class} = \langle dN_{ch}/d\eta \rangle_{\min} < \langle dN_{ch}/d\eta \rangle \leq \langle dN_{ch}/d\eta \rangle_{\max}. \quad (2)$$

The multiplicity ranges of each class used in this study are listed in Table 3.

**Table 3.** Multiplicity classes used in HIJING++ runs.

| Class                                  | I  | II | III | IV | V  | VI | VII | VIII | IX | X  | XI | XII | XIII | XIV | XV  |
|--|----|----|-----|----|----|----|-----|------|----|----|----|-----|------|-----|-----|
| $\langle dN_{ch}/d\eta \rangle_{\min}$ | 0  | 10 | 15  | 20 | 25 | 30 | 35  | 40   | 45 | 50 | 55 | 60  | 70   | 80  | 90  |
| $\langle dN_{ch}/d\eta \rangle_{\max}$ | 10 | 15 | 20  | 25 | 30 | 35 | 40  | 45   | 50 | 55 | 60 | 70  | 80   | 90  | 100 |

Using this event classification, we calculated the mid-rapidity transverse momentum spectra of charge averaged pions, kaons, and protons in  $INEL > 0$  events. We generated 200M events. To avoid superfluous overcrowding of the available space, we show only the low, moderate, and high multiplicity spectra along with the fitted Tsallis–Pareto curves defined by Equation (1) in Figure 4.

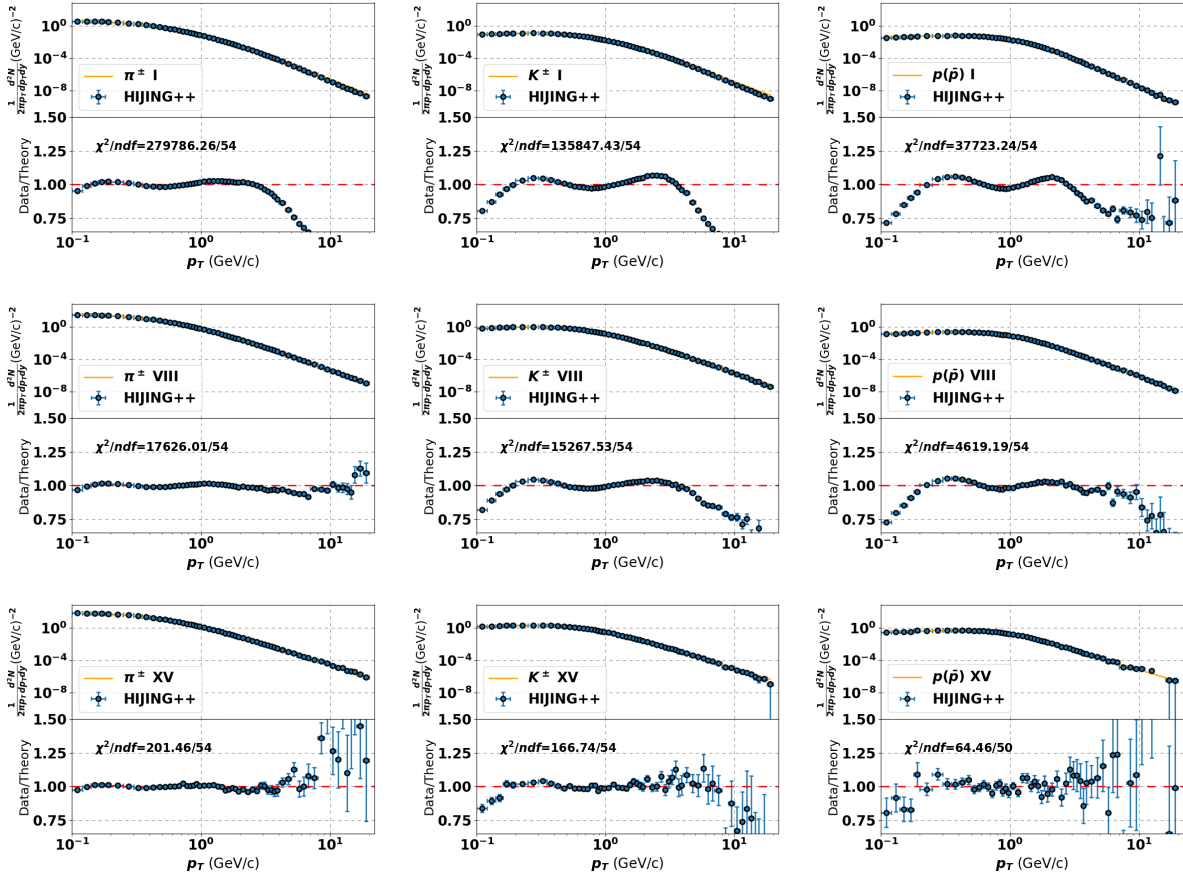


**Figure 4.** Calculated  $p_T$  spectra of charge averaged pions (**left column**), kaons (**middle column**), and protons (**right column**) at low (**top row**), moderate (**middle row**), and high (**bottom row**) multiplicity classes as blue dots and the fitted Equation (1) Tsallis–Pareto curve (orange line). The lower part of each panel shows the  $Data/Theory$  ratio.

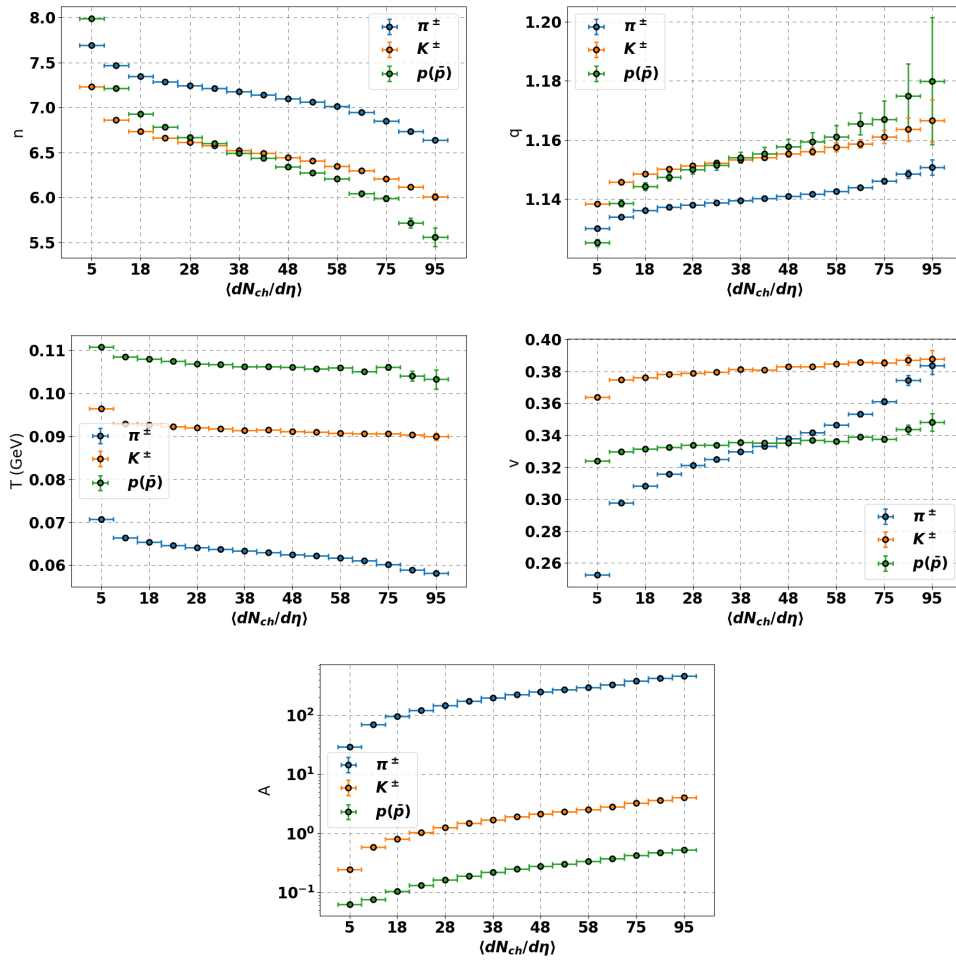
In Figure 4, we can see that the best fits occurred at the high multiplicity events. For the pions, the fitted curves follow the points well at the low- $p_T$  region, while for the kaons and protons with higher mass at the low- $p_T$  region the model overpredicts the yield. We note, however, that for the HIJING++ run we investigated the same  $0.1 \text{ GeV}/c < p_T < 20 \text{ GeV}/c$  region for all hadrons, while the low- $p_T$  part for the kaons and protons in the case of the experimental results is missing. At the high- $p_T$  region, the fit breaks down because of the low statistics.

In Figure 5, the fitted parameters in the function of the event multiplicity are shown. Using the distribution form Equation (1), we observe that with increasing multiplicity the  $q$  parameter increases for each hadron but with different slopes: the increase of  $q$  (or the decrease of  $n$ ) is the largest for the heaviest hadron. On the other hand, the temperature decreases slowly with the increasing pseudorapidity density. Here, the previously observed  $T_{\pi^\pm} < T_{K^\pm} < T_{p(\bar{p})}$  mass hierarchy stays valid with the multiplicity averaged values, as can be seen in Table 4.

**Table 4.** The multiplicity averaged temperature parameters for charge averaged pions, kaons, and protons.

| Hadron       | $\langle T_i \rangle$ (GeV) |
|--------------|-----------------------------|
| $\pi^\pm$    | $0.063 \pm 0.003$           |
| $K^\pm$      | $0.092 \pm 0.001$           |
| $p(\bar{p})$ | $0.106 \pm 0.002$           |

The radial flow velocity also increases with the multiplicity, but also with different rates. While at low multiplicity the lightest pions have the smallest  $v$ , it increases rapidly with the increasing multiplicity. On the other hand, the rate of increase in the case of protons and kaons are approximately the same. These observations require further investigation. Finally, the amplitudes are increasing for each hadron species with the multiplicity. The value of pions is much higher than those of the heavier hadrons, which indicates that with increasing multiplicity the number of the produced pions grows faster than the number of kaons and protons.

**Figure 5.** The fitted parameters of the Tsallis-Pareto distribution defined by Equation (1), in the function of the event multiplicity class defined as in Table 3.

## 5. Conclusions

In this contribution, we investigated the multiplicity dependence of the parameters of the non-extensive hadronization model in proton–proton collisions using HIJING++ calculations. We presented the current status of the tuning process of HIJING++ and showed that it is able to reproduce the main high-energy physics observables such as multiplicity and  $p_T$  distributions. We presented the non-extensive hadronization model that we used to describe the transverse momentum distribution of identified hadrons. In accordance with our previous results, we showed that a mass hierarchy emerges in the Tsallis parameters. Utilizing the tuned HIJING++ calculations, we also extracted the parameters from  $\sqrt{s} = 7$  TeV proton–proton collisions Monte Carlo calculations with various event multiplicity classifications. Our study showed that the  $q$  non-extensivity parameter increases with increasing multiplicity, while the  $T$  temperature has only a slight decrease. On the other hand, all hadrons result in a non-zero, increasing radial flow velocity. All parameters show the earlier observed mass hierarchy. Our findings suggest that these parameters are sensitive to the event size and may serve as a thermometer of the collision.

**Author Contributions:** Software and formal analysis: G.B. and G.P.; investigation: G.B. and G.G.B.; writing—original draft preparation: G.B.; writing—review and editing: G.G.B.; supervision: G.G.B., T.S.B., and G.P.; funding acquisition: G.G.B. and T.S.B.

**Funding:** This research was funded by Hungarian-Chinese cooperation grant No. MOST 2014DFG02050, the Wigner HAS-OBOR-CCNU grant, and OTKA grants K120660 and K123815. G.B. acknowledges the support of the Wigner Data Center and Wigner GPU Laboratory.

**Conflicts of Interest:** The authors declare no conflict of interest.

## References

1. Bíró, G.; Barnaföldi, G.G.; Biró, T.S.; Ürmössy, K.; Takács, Á. Systematic Analysis of the Non-extensive Statistical Approach in High Energy Particle Collisions—Experiment vs. Theory. *Entropy* **2017**, *19*, 88, doi:10.3390/e19030088.
2. Grigoryan, S. Using the Tsallis distribution for hadron spectra in  $pp$  collisions: Pions and quarkonia at  $\sqrt{s} = 5$ –13000 GeV. *Phys. Rev. D* **2017**, *95*, 056021, doi:10.1103/PhysRevD.95.056021.
3. Zheng, H.; Zhu, L.; Bonasera, A. Systematic analysis of hadron spectra in p+p collisions using Tsallis distributions. *Phys. Rev. D* **2015**, *92*, 074009, doi:10.1103/PhysRevD.92.074009.
4. Wong, C.Y.; Wilk, G.; Cirto, L.J.L.; Tsallis, C. Possible Implication of a Single Nonextensive  $p_T$  Distribution for Hadron Production in High-Energy  $pp$  Collisions. *Eur. Phys. J. Web Conf.* **2015**, *90*, 04002, doi:10.1051/epjconf/20159004002.
5. Tripathy, S.; Bhattacharyya, T.; Garg, P.; Kumar, P.; Sahoo, R.; Cleymans, J. Nuclear Modification Factor Using Tsallis Non-extensive Statistics. *Eur. Phys. J. A* **2016**, *52*, 289, doi:10.1140/epja/i2016-16289-4.
6. Bhattacharyya, T.; Cleymans, J.; Marques, L.; Mogliacci, S.; Paradza, M.W. On the precise determination of the Tsallis parameters in proton–proton collisions at LHC energies. *J. Phys. G: Nucl. Part. Phys.* **2018**, *45*, 055001, doi:10.1088/1361-6471/aaea0.
7. Shen, K.; Barnaföldi, G.G.; Biró, T.S. Hadronization within Non-Extensive Approach and the Evolution of the Parameters. *arXiv* **2019**, arXiv:1905.05736.
8. Bíró, G.; Barnaföldi, G.G.; Biró, T.S.; Shen, K. Mass hierarchy and energy scaling of the Tsallis–Pareto parameters in hadron productions at RHIC and LHC energies. *Eur. Phys. J. Web Conf.* **2018**, *171*, 14008, doi:10.1051/epjconf/201817114008.
9. Bíró, G.; Barnaföldi, G.G.; Biró, T.S.; Ürmössy, K. Application of the Non-extensive Statistical Approach to High Energy Particle Collisions. *AIP Conf. Proc.* **2017**, *1853*, 080001, doi:10.1063/1.4985366.
10. Barnaföldi, G.G.; Ürmössy, K.; Bíró, G. A ‘soft+hard’ model for Pion, Kaon, and Proton Spectra and  $v_2$  measured in PbPb Collisions at  $\sqrt{s} = 2.76$  ATeV. *J. Phys. Conf. Ser.* **2015**, *612*, 012048, doi:10.1088/1742-6596/612/1/012048.



11. Takacs, A.; Barnaföldi, G.G. Non-extensive Motivated Parton Fragmentation Functions. *Proceedings* **2019**, *10*, 12, doi:10.3390/proceedings2019010012.
12. Khuntia, A.; Sharma, H.; Kumar Tiwari, S.; Sahoo, R.; Cleymans, J. Radial flow and differential freeze-out in proton–proton collisions at  $\sqrt{s} = 7$  TeV at the LHC. *Eur. Phys. J. A* **2019**, *55*, 3, doi:10.1140/epja/i2019-12669-6.
13. Wilk, G.; Włodarczyk, Z. Some intriguing aspects of multiparticle production processes. *Int. J. Mod. Phys. A* **2018**, *33*, 1830008, doi:10.1142/S0217751X18300089.
14. Urmosy, K.; Biro, T.S. Cooper-Frye Formula and Non-extensive Coalescence at RHIC Energy. *Phys. Lett. B* **2010**, *689*, 14, doi:10.1016/j.physletb.2010.04.037.
15. Van, P.; Barnafoldi, G.G.; Biro, T.S.; Urmosy, K. Nonadditive thermostatistics and thermodynamics. *J. Phys. Conf. Ser.* **2012**, *394*, 012002, doi:10.1088/1742-6596/394/1/012002.
16. Shen, K.; Biro, T.S.; Wang, E. Different Non-extensive Models for heavy-ion collisions. *Physica A* **2018**, *492*, 2353–2360, doi:10.1016/j.physa.2017.11.160.
17. Wang, X.N.; Gyulassy, M. HIJING: A Monte Carlo model for multiple jet production in pp, pA, and AA collisions. *Phys. Rev. D* **1991**, *44*, 3501–3516.
18. Deng, W.T.; Wang, X.N.; Xu, R. Hadron production in p+p, p+Pb, and Pb+Pb collisions with the hijing 2.0 model at energies available at the CERN Large Hadron Collider. *Phys. Rev. C* **2011**, *83*, 014915.
19. Barnaföldi, G.G.; Bíró, G.; Gyulassy, M.; Haranóz, S.M.; Lévai, P.; Ma, G.; Papp, G.; Wang, X.N.; Zhang, B.W. First Results with HIJING++ in High-Energy Heavy-Ion Collisions. *Nucl. Part. Phys. Proc.* **2017**, *289–290*, 373, doi:10.1016/j.nuclphysbps.2017.05.086.
20. Papp, G.; Barnaföldi, G.G.; Bíró, G.; Gyulassy, M.; Harangozó, S.M.; Ma, G.; Lévai, P.; Wang, X.N.; Zhang, B.W. First Results with HIJING++ on High-energy Heavy Ion Collisions. *arXiv* **2018**, arXiv:1805.02635.
21. Albacete, J.L.; Arleo, F.; Barnaföldi, G.G.; Bíró, G.; d’Enterria, D.; Ducloué, B.; Eskola, K.J.; Ferreiro, E.G.; Gyulassy, M.; Harangozó, S.M.; et al. Predictions for Cold Nuclear Matter Effects in p+Pb Collisions at  $\sqrt{s_{NN}} = 8.16$  TeV. *Nucl. Phys. A* **2018**, *972*, 18–85, doi:10.1016/j.nuclphysa.2017.11.015.
22. Bíró, G.; Papp, G.; Barnaföldi, G.G.; Nagy, D.; Gyulassy, M.; Lévai, P.; Wang, X.N.; Zhang, B.W. HIJING++, a Heavy Ion Jet Interaction Generator for the High-luminosity Era of the LHC and Beyond. *Proceedings* **2019**, *10*, 4, doi:10.3390/proceedings2019010004.
23. Sjöstrand, T.; Ask, S.; Christiansen, J.R.; Corke, R.; Desai, N.; Ilten, P.; Mrenna, S.; Prestel, S.; Rasmussen, C.O.; Skands, P.Z. An Introduction to PYTHIA 8.2. *Comput. Phys. Commun.* **2015**, *191*, 159–177.
24. Buckley, A.; Ferrando, J.; Lloyd, S.; Nordström, K.; Page, B.; Rüfenacht, M.; Schönherr, M.; Watt, G. LHAPDF6: Parton density access in the LHC precision era. *Eur. Phys. J. C* **2015**, *75*, 132.
25. Galassi, M.; Davies, J.; Theiler, J.; Gough, B.; Jungman, G.; Alken, P.; Booth, M.; Rossi, F.; Ulerich, R. *GNU Scientific Library Reference Manual*, 3rd ed.; Network Theory Limited: London, UK. ISBN 0954612078
26. Lepage, G.P. A new algorithm for adaptive multidimensional integration. *J. Comp. Phys.* **1978**, *27*, 192–203.
27. ROOT Data Analysis Framework. Available online: <https://root.cern.ch/> (accessed on 30 April 2019).
28. Dulat, S.; Hou, T.J.; Gao, J.; Guzzi, M.; Huston, J.; Nadolsky, P.; Pumplin, J.; Schmidt, C.; Stump, D.; P. Yuan, C. New parton distribution functions from a global analysis of quantum chromodynamics. *Phys. Rev. D* **2016**, *93*, 033006.
29. Eskola, K.J.; Paakkinen, P.; Paukkunen, H.; Salgado, C.A. EPPS16: Nuclear parton distributions with LHC data. *Eur. Phys. J. C* **2017**, *77*, 163.
30. Buckley, A.; Hoeth, H.; Lacker, H.; Schulz, H.; von Seggern, J.E. Systematic event generator tuning for the LHC. *Eur. Phys. J. C* **2010**, *65*, 331, doi:10.1140/epjc/s10052-009-1196-7.
31. Tange, O. GNU Parallel: The Command-Line Power Tool. Available online: <https://www.usenix.org/system/files/login/articles/105438-Tange.pdf> (accessed on 26 May 2019).
32. Adam, J.; Adamová, D.; Aggarwal, M.M.; Rinella, G.A.; Agnello, M.; Agrawal, N.; Ahammed, Z.; Ahmad, S.; Ahn, S.U.; Aiola, S.; et al. Multiplicity dependence of charged pion, kaon, and (anti)proton production at large transverse momentum in p-Pb collisions at  $\sqrt{s_{NN}} = 5.02$  TeV. *Phys. Lett. B* **2016**, *760*, 720–735, doi:10.1016/j.physletb.2016.07.050.

33. Aamodt, K.; Abel, N.; Abeyssekara, U.; Quintana, A.A.; Abramyan, A.; Adamova, D.; Aggarwal, M.M.; Rinella, G.A.; Agocs, A.G.; Salazar, S.A.; et al. Charged-particle multiplicity measurement in proton–proton collisions at  $\sqrt{s} = 7$  TeV with ALICE at LHC. *Eur. Phys. J. C* **2010**, *68*, 345, doi:10.1140/epjc/s10052-010-1350-2.
34. Acharya, S.; Adamová, D.; Adolfsson, J.; Aggarwal, M.M.; AglieriRinella, G.; Agnello, M.; Agrawal, N.; Ahammed, Z.; Ahmad, N.; Ahn, S.U.; et al. Charged-particle multiplicity distributions over a wide pseudorapidity range in proton–proton collisions at  $\sqrt{s} = 0.9, 7,$  and 8 TeV. *Eur. Phys. J. C* **2017**, *77*, 852, doi:10.1140/epjc/s10052-017-5412-6.

35. Wilk, G.; Włodarczyk, Z. Tsallis Distribution Decorated With Log-Periodic Oscillation. *Entropy* **2015**, *17*, 384, doi:10.3390/e17010384.
36. Rybczyński, M.; Wilk, G.; Włodarczyk, Z. System size dependence of the log-periodic oscillations of transverse momentum spectra. *Eur. Phys. J Web Conf.* **2015**, *90*, 01002, doi:10.1051/epjconf/20159001002.